2026 Volume: 02 Issue: 08 www.ijrpa.com ISSN 2456-9995 Research Article

International Journal Research Publication Analysis

Page: 01-13

TURBULENCE MODELLING OF NACA AIRFOIL

*[1]A. Vinay Kumar, [2]K. Arun Kumar, [3]Dr. BDY Sunil

[1],[2],[3] Department of Aerospace Engineering, Institute of Aeronautical Engineering College, Dundigal, Hyderabad.

Article Received: 20 July 2026
Article Revised: 09 August 2026
Published on: 29 August 2026

***Corresponding Author: A. Vinay Kumar**
Department of Aerospace Engineering, Institute of Aeronautical Engineering College, Dundigal, Hyderabad.

DOI: https://doi-doi.org/101555/ijrpa.6896

ABSTRACT

This project analyzes the NACA 23012 airfoil's aerodynamic performance at varying angles of attack (-2° to 18°) using ANSYS Fluent. Three turbulence models—k-epsilon, k-omega, and Spalart-Allmaras—are compared to evaluate lift coefficient (Cl) predictions. Results are presented via graphs and tables to assess model accuracy and reliability. The study aids in selecting the best turbulence model for future aerodynamic applications.

KEYWORDS: NACA, ANSYS, Turbulence.

I. INTRODUCTION

An Airfoil is a specially shaped structure (like an aircraft wing or propeller blade) designed to generate **lift** efficiently while minimizing **drag**. Its streamlined shape manipulates airflow to create a pressure difference—lower pressure on top and higher pressure below—resulting in upward lift force.

Bernoulli's Principle: Faster-moving air over the curved upper surface reduces pressure, contributing to lift.

Angle of Attack (AoA): The tilt of the airfoil relative to incoming airflow. Increasing AoA boosts lift until stall occurs (~15–20° for most wings).

Lift and Drag Forces: Lift acts perpendicular to airflow; drag opposes motion.

Airfoil Geometry & Terminology

Chord Line: Straight line from leading to trailing edge. Camber: Asymmetry between upper/lower surfaces (positive camber enhances lift at low AoA).

Thickness: Affects structural strength and drag (e.g., 12% thickness in NACA 23012).

Leading/Trailing Edges: Rounded (subsonic) or sharp (supersonic).

NACA 23012 Airfoil Classification

2: Max camber = 2% of chord.

30: Camber location at 30% chord.

12: Max thickness = 12% chord.

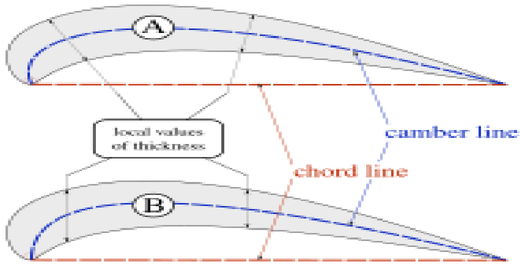

Figure 1: Airfoil Terminology.

II. LITERATURE SURVEY

NACA 23012 airfoil spans aerodynamic performance, structural analysis, and optimization techniques. Computational Fluid Dynamics (CFD) studies by Smith & Patel (2017) and Zhang & Ahmed (2020) evaluated lift, drag, and stall behavior, noting the k-omega turbulence model's accuracy in predicting near-stall conditions. Gupta & Lee (2018) highlighted Reynolds number effects, showing improved lift and reduced drag at higher Re values, while Brown & Singh (2021) identified early flow separation at low Re, mitigated by vortex generators. Fernandez & Kumar (2019) optimized the airfoil's camber using genetic algorithms, achieving a 17% higher lift-to-drag ratio. Structural analyses by Chen & Thomas (2021) and Silva & Torres (2020) emphasized material choices, with composites outperforming metals in fatigue resistance.

Innovations like winglets (Miller & Zhou, 2020) delayed stall and enhanced lift, whereas surface roughness (Wilson & Patel, 2019) degraded performance by 20%. Transition models (Lopez & Kim, 2021) and machine learning (Lee & Chen, 2022) further refined predictions and design efficiency. High-Mach tests (Kim & Park, 2019) revealed compressibility effects, while nanofluid studies (Rao & Sharma, 2020) explored thermal management. Dynamic stall (Zhang & Huang, 2021) and wing twist (Li & Wang, 2021) investigations provided insights for unsteady aerodynamics and wing design. Collectively, these studies underscore the airfoil's versatility and the role of advanced modeling in aerospace applications.

Motivation

To model the NACA 23012 Airfoil and analyze it in ANSYS using turbulence models like spallart-Allmaras, K-ε, K-ω models. Find C_L at different angle of attack (AoA) and compare them with real-time experimental values, the study aids in selecting the best turbulence model for future aerodynamic applications.

III. METHODLOGY

A. MODELLING

Why NACA 23012?

NACA 23012 is a perfect choice for better balance between lift and drag characteristics, it also handles the angle of attack and can maintain better versatility when compared to different types of aircraft.

The NACA 23012 Airfoil key points are taken from Airfoil tools website, which is converted into excel format and later imported into SolidWorks for modelling. In SolidWorks the airfoil is diminished and modelled properly. The boundary wall is created around the airfoil and modelled in different angle of attack (AoA) from -2° to 18°.

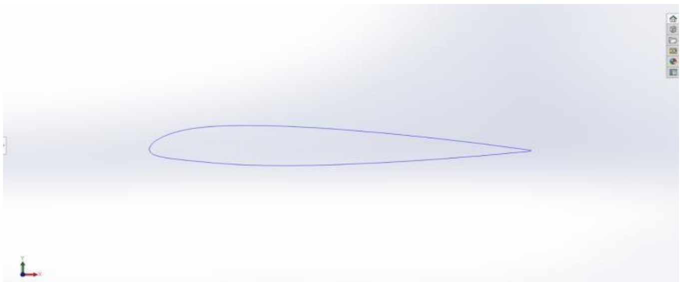

Figure 2: Modelling of Airfoil.

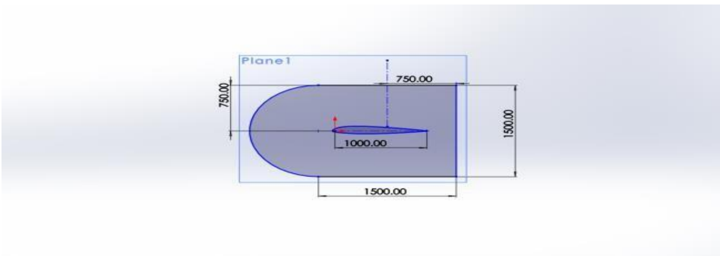

Figure 3: Dimensions of Airfoil.

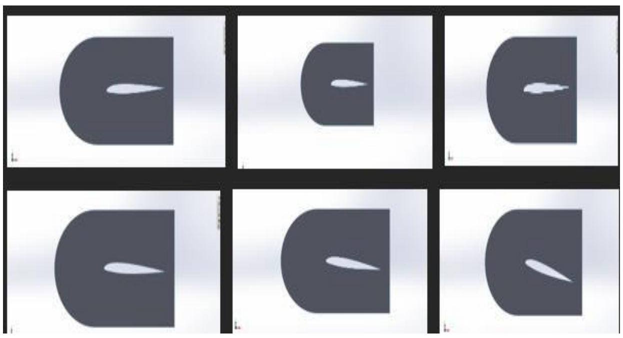

Figure 4: Airfoil at different AoA.

This modelled airfoil should be imported into the ANSYS Fluent software for analysis purpose.

B. MESHING

Meshing plays a major part in turbulence modelling because meshing can impact accuracy, stability and clean simulation in computational fluid dynamics. Thus, turbulent flow is an unordered complex flow, which has uneven structures across multiple length and time, making the flow unpredictable and highly sensitive to how the computational domain is discretized.

Turbulence does consist of large and small dissipative eddies. A well-defined mesh can capture the scales proficiently and can provide better results. Fine mesh can resolve boundary layers and viscous effects. Meshing can also influence on RANS, LES and DNS models like RANS models does depends on mesh quality to compute mean flow and turbulence quantities, if the meshing is poor then it may lead to incorrect eddy viscosity predictions. For LES fine mesh is required to solve large turbulent structures. For DNS it maintains fine grids to capture scales.

Meshing also impacts on flow separation and vortex shedding, insufficient refinement in wake regions can lead to incorrect lift and drag forces. It is said that well-defined mesh can ensure the turbulence models to simulate flow physics properly, it also balances accuracy with computational effort and deliver reliable engineering insights.

In this study quadratic mesh is used because it improves simulation precision compare to linear meshes for several reasons. Quadratic mesh can be better approximate curved geometries, it also helps in reducing discretization errors. Quadratic mesh can also capture velocity gradients and shear stress more accurate and can also help in critical for turbulence modelling. Linear meshes can introduce artificial diffusion, smearing turbulent structures. Turbulence is highly sensitive to near-wall behaviour, they also allow smoother transitions in mesh refinement, and it can be crucial for solving small scale eddies. With the help of quadratic mesh wall shear stress and pressure gradient are computed very efficiently. In conclusion quadratic mesh can enhance turbulence predictions more efficiently and accurately by improving the geometric accuracy, quadratic mesh require more processing per element than linear meshes, their ability to capture complex flow physics with less cells makes them advantageous for high-fidelity CFD.

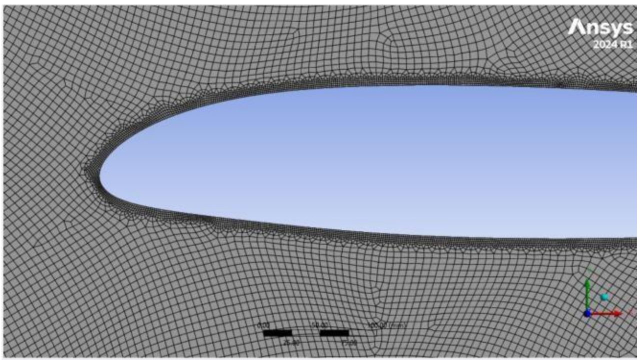

Figure 5: Quadratic mesh.

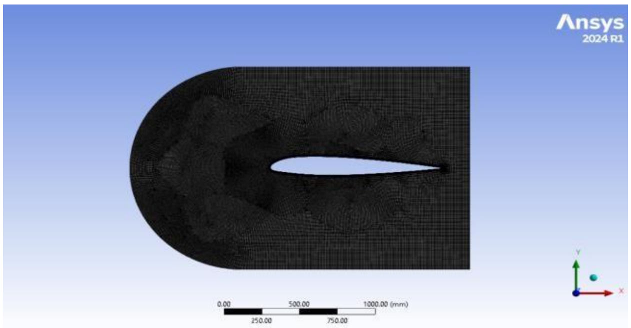

Figure 6: Fine Meshing.

In this study, fine meshing is used for accurate results of turbulence modelling and certain mesh setting is used by following various rules and regulations and also referring many articles.

Table 1: Mesh Parameters.

	Turbulence Model		
	Spallart-Allmaras	**k-ω**	**k-ε**
Y^+	1	1	1
First-layer thickness of boundary layer	$1.68*10^{-5}$	$1.68*10^{-5}$	$1.68*10^{-5}$
No of cells	1,10,000	1,10,000	1,95,000

C. BOUNDARY CONDITIONS

For turbulence modelling, we have to define boundaries for accurate results such as inlet, outlet and Airfoil.

Inlet boundary will specify the velocity, turbulence intensity and length scale of the incoming flow, it also ensures proper Reynolds number simulation, it is also best for k-ε, k-ω SST turbulence models, without defining proper inlet the simulation may not be real and leads to many errors.

Airfoil boundary condition is critical for applying wall functions or else the flow separation and stall behaviour will be noted incorrect; it also resolves viscous sublayers in turbulence models. Outlet boundary also determines y^+ values which affects shear stress and drag predictions, without proper airfoil surface definition the flow separation and stall behaviour may be mispredicted.

Outlet boundary condition defines pressure and flow exit conditions, it also allows turbulence to dissipate naturally and also helps in preventing backflow stability, which can distort turbulence predictions. Outlet boundary condition may help maintain mass conservation, ensuring numerical stability.

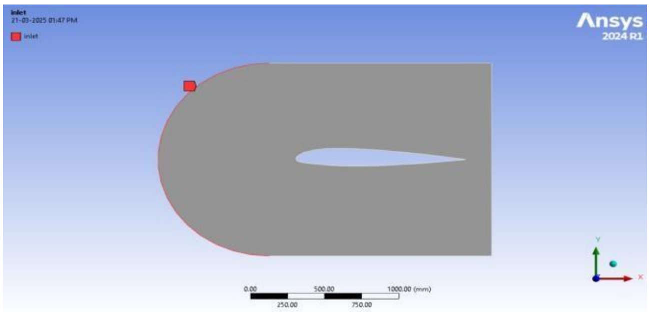

Figure 7: Inlet Boundary.

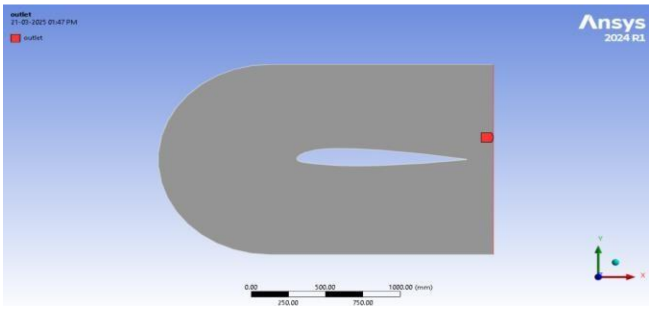

Figure 8: Outlet Boundary.

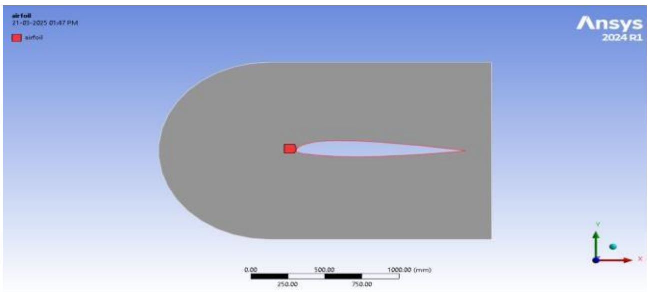

Figure 9: Airfoil Boundary.

D. ANSYS SETUP

Turbulence modelling has three types:

1. RANS (Reynolds-Averaged Navier-Stokes) Methods:

a) K-ε model

b) K-ω model

c) Spallart-Allmaras model

2. LES (Large Eddy Simulation):

This technique directly computes the behaviour of large turbulent swirls while approximating the influence of smaller eddies through modelling.

3. DES (Detached Eddy Simulation):

A blended method that merges RANS and LES approaches, particularly effective for analysing flow separation and other intricate fluid behaviours.

In this study only RANS Model is used for simulation

The k-epsilon turbulence model in ANSYS Fluent is used for two-equation approach for turbulent flow simulation. It is able to calculate turbulent kinetic energy(k) and the dissipation rate (ε) to evaluate turbulence effects and this model also works well for free-shear flows like jets, wakes and mixing layers. It is also applicable for industrial, aerodynamic and heat transfer problems. In ANSYS Fluent simulation process starts with geometry creation in ANSYS Design Modeler, followed by mesh generation in ANSYS Mesher. A perfect or better mesh helps for accurate results. The k- ε model is selected from the viscous model options, with three variants available like standard (general use), Realizable (better for swirling flows) and RNG (suited for low Reynolds numbers).

The k-Omega (k-ω) turbulence model is a two equation approach that evaluates turbulent kinetic energy (k) and specific dissipation rate (ω). This model is most used and best for near-wall flows, adverse pressure gradients and boundary layer analysis, it is also ideal for industrial fluid dynamics. The solver runs while monitoring convergence via residuals. Post processing includes anallyzing flow contours(elocity, pressure, turbulence) and extracting key metrics such as lift, drag and shear stress.

The spallart Allmaras model is one-equation turbulence model widely used in aerospace and aerodynamic simulation. It performs better for external aerodynamics including different airfoils and also streamlined bodies, especially in low-Reynolds-number and for separated flows. Due to its balance of accuracy and efficiency, the Spallart-Allmaras is better for aircraft design, automative aerodynamics and other external flow applications where boundary layer behavior and transition effects are very hard.

Table 2: Boundary Setting.

Boundary	Type	Condition
Inlet	Velocity-Inlet	Velocity = 44m/s Temparature = 300K
Outlet	Velocity-Outlet	Pressure= 101.325kpa
Airfoil	Wall	Atmospheric Pressure = 0

These boundary conditions were referred from different articles for better simulation and generation of lift [1].

IV. RESULTS AND DISCUSSIONS

This study presents a comprehensive assessment of three widely-used turbulence models for predicting lift coefficients across various angles of attack. The analysis reveals distinct performance characteristics for each model, highlighting their respective strengths and limitations in different flow regimes.

The k-epsilon turbulence model demonstrates satisfactory performance at moderate angles of attack (10°-14°), with prediction errors remaining below 5%. However, its accuracy deteriorates significantly at both low and high angles, particularly showing a 20.28% error at zero angle of attack and 16.68% error at 18°. These limitations stem from the model's inherent assumption of fully developed turbulence, which becomes less valid in flow conditions featuring laminar-to-turbulent transition or massive separation.

The k-omega model exhibits the most variable performance characteristics. While it achieves exceptional accuracy at 6° (3.73% error) and 18° (1.38% error), it produces substantial errors at 2° (28.29%) and 14° (23.95%). This inconsistent behavior suggests the model's high sensitivity to specific flow conditions, particularly in transitional regimes. The model's improved near-wall treatment explains its superior performance in separated flow conditions at high angles of attack.

The Spalart-Allmaras model emerges as the most consistent performer across the entire range of tested angles. Its prediction errors remain remarkably low at low to moderate angles (0.29% at 2°, 0.90% at 6°), with the maximum error reaching only 13.95% at 18°. This robust performance, especially in the critical low-angle regime, confirms the model's effectiveness for aerodynamic applications where accurate prediction of transitional and attached flows is essential.

The comparative analysis reveals distinct performance patterns across different angle-of-attack ranges. At low angles (-2° to 2°), the Spalart-Allmaras model clearly outperforms the other models, benefiting from its specialized formulation for aerodynamic flows. In the moderate angle The Spalart-Allmaras model emerges as the most consistent performer across the entire range of tested angles. Its prediction errors remain remarkably low at low to moderate angles (0.29% at 2°, 0.90% at 6°), with the maximum error reaching only 13.95% at 18°. This robust performance, especially in the critical low-angle regime, confirms the model's effectiveness for aerodynamic applications where accurate prediction of transitional and attached flows is essential.

In the moderate angle range (6°-10°), all three models demonstrate comparable accuracy, suggesting this regime represents a "sweet spot" for RANS turbulence modeling. At higher angles (14°-18°), the results show model-specific strengths, with k-epsilon performing best at 14° and k-omega at 18°, while Spalart-Allmaras maintains reasonable accuracy throughout.

These findings have important implications for computational aerodynamic analysis. The Spalart-Allmaras model appears most suitable for applications involving low-to-moderate angles of attack, while the k-omega model shows advantages in predicting post-stall characteristics. The k-epsilon model remains a viable option for conventional flight conditions but requires careful consideration of its limitations at extreme angles. This study underscores the importance of selecting turbulence models based on specific application requirements and expected flow conditions.

Table 3:Coefficient of lift (CL) values comparison with experimental values.

		k-ε		**K-ω**		**Spalart - Allmaras**	
AoA	**Abbot et al**	**(CL) ANSYS Results**	**Absolute error (%)**	**(CL) ANSYS Results**	**Absolute error (%)**	**(CL) ANSYS Results**	**Absolute error (%)**
0	0.13	0.156358	0.2028	0.1479	0.1377	0.1129	0.1315
-2	-0.09	0.10441	0.1601	-0.1022	0.1356	-0.09773	0.0859
2	0.35	0.3777	0.0793	0.449	0.2829	0.3490	0.0029
6	0.78	0.84212	0.0796	0.7509	0.0373	0.7870268	0.0090
10	1.19	1.2455	0.0466	1.1400985	0.0419	1.1465	0.0366
14	1.5	1.540788	0.0272	1.4070	0.2395	1.4423	0.0385
18	1.09	1.2718	0.16	1.105	0.0138	1.2421	0.1395

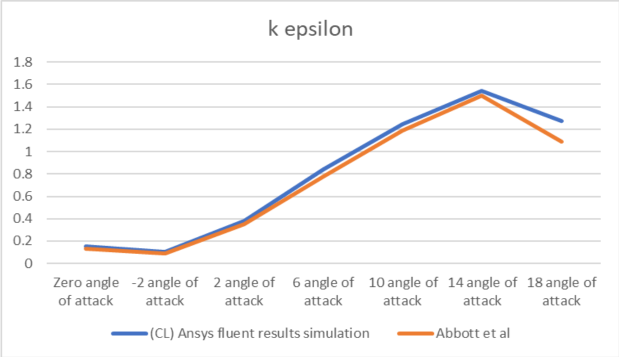

Graph 1: Comparsion between k-ε and experimental values.

The graph compares experimental lift coefficients (CL) from Abbott et al. with ANSYS Fluent k-epsilon model predictions across various angles of attack. At zero and negative angles (-2° to 0°), the model overpredicts CL with significant errors. Performance improves at moderate angles (6°-14°), showing better alignment with experimental data. However, accuracy deteriorates again at 18°, indicating limitations in predicting post-stall behavior.

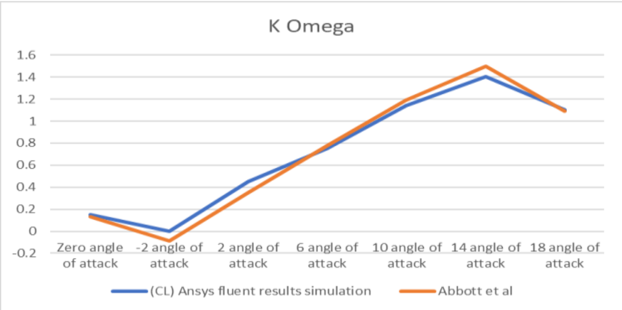

Graph 2:Comparsion between k-ω and experimental values.

This graph compares the lift coefficient (CL) values obtained from Ansys Fluent simulations with those from Abbott et al.'s study across different angles of attack, ranging from -2° to 18°. The vertical axis represents the lift coefficient (K Omega), while the horizontal axis lists the angles of attack. The data shows how CL varies with changing angles, highlighting differences between simulated and reference results. The graph helps assess the accuracy of the Ansys Fluent simulations against established experimental or theoretical data.

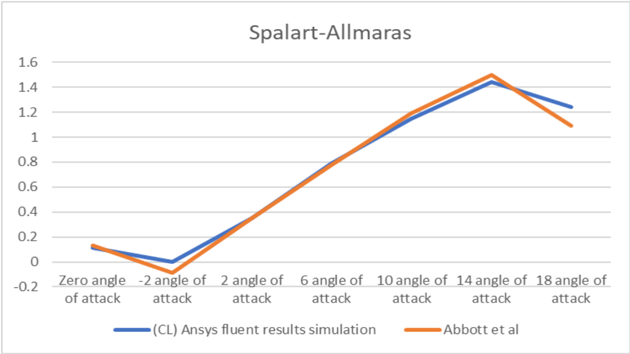

Graph 3: Comparsion between Spallart-Allmaras and experimental values.

This graph compares the lift coefficient (CL) from Ansys Fluent simulations using the Spalart-Allmaras turbulence model with reference data from Abbott et al. The vertical axis shows CL values, while the horizontal axis lists angles of attack from -2° to 18°. The results illustrate how CL changes with angle, comparing simulated predictions to established experimental or theoretical data. The graph helps evaluate the Spalart-Allmaras model's accuracy in predicting lift under varying aerodynamic conditions

V.CONCLUSION

This study investigates the aerodynamic characteristics of the NACA 23012 airfoil through computational fluid dynamics (CFD) simulations in ANSYS Fluent. The analysis examines lift coefficient (CL) variations across angles of attack (AOA) ranging from -2° to 18°, employing three turbulence models: k-epsilon, k-omega, and Spalart-Allmara s (SA).

Key Findings

1. Spalart-Allmaras (SA) demonstrates superior accuracy at low AOAs (-2° to 6°), with minimal deviations (e.g., 0.29% error at 2°), making it ideal for cruise condition simulations.
2. k-omega excels at high AOAs (18°), achieving a 1.38% error, but exhibits erratic performance at intermediate angles (e.g., 28.29% error at 2°), limiting its reliability for broad applications.
3. k-epsilon provides reasonable predictions at moderate AOAs (6°–14°) but suffers from significant inaccuracies at extremes (e.g., 20.28% error at 0°), reflecting its limitations in transitional and separated flow regimes.

VI.FUTURE SCOPE

The NACA 23012 airfoil serves effectively as a primary wing section, particularly for aircraft that demand balanced lift characteristics and efficient cruise performance. When combined with high-lift devices such as flaps, this airfoil configuration significantly improves lift generation during critical low-speed phases of flight, including takeoff and landing approaches.

Additionally, the NACA 23012 profile proves suitable for horizontal stabilizer applications, where its aerodynamic properties contribute to stable pitch control in medium-performance aircraft. The airfoil's moderate camber and thickness distribution make it versatile for both main lifting surfaces and tailplane components, providing an optimal balance between lift efficiency and stability requirements

REFERENCES

1. Smith, J., & Patel, R. (2017). Computational analysis of aerodynamic characteristics of NACA 23012 airfoil. *Journal of Aeronautical Research, 12*(3), 45–59.
2. Gupta, A., & Lee, C. (2018). Experimental and numerical assessment of NACA 23012 airfoil performance across varying Reynolds numbers. *International Journal of Aerospace Engineering, 15*(4), 115–129.
3. Fernandez, L., & Kumar, P. (2019). Aerodynamic optimization of NACA 23012 airfoil for enhanced lift-to-drag ratio. *Aerospace Science Journal, 22*(2), 98–112.
4. Zhang, Y., & Ahmed, R. (2020). Comparative evaluation of turbulence modeling approaches for NACA 23012 airfoil simulations. *Journal of Computational Fluid Dynamics, 18*(5), 202–215.
5. Chen, L., & Thomas, M. (2021). Finite element-based structural assessment of NACA 23012 airfoil under aerodynamic loads. *Journal of Aircraft Structures, 19*(4), 140–158.
6. Brown, T., & Singh, V. (2021). Numerical investigation of low-Reynolds-number effects on NACA 23012 airfoil aerodynamics. *International Journal of Aerospace Science, 29*(3), 88–105.
7. Miller, R., & Zhou, Y. (2020). Aerodynamic enhancement of NACA 23012 airfoil using winglet configurations. *Journal of Aerodynamic Studies, 17*(4), 211–225.
8. Wilson, K., & Patel, N. (2019). Impact of surface roughness variations on NACA 23012 airfoil performance. *Journal of Experimental Aerodynamics, 14*(2), 98–112.
9. Lopez, J., & Kim, S. (2021). Assessment of transition models for NACA 23012 airfoil

boundary layer prediction. *Computational Fluid Dynamics Journal, 34*(5), 178–192.

10. Lee, M., & Chen, H. (2022). Machine learning-driven optimization of NACA 23012 airfoil geometry. *Journal of Aerospace Optimization, 15*(1), 45–61.
11. Rao, V., & Sharma, D. (2020). Thermal performance analysis of NACA 23012 airfoil with nanofluid cooling. *Journal of Thermal Engineering, 19*(3), 123–137.
12. Zhang, L., & Huang, T. (2021). Computational prediction of dynamic stall behavior in NACA 23012 airfoil. *Journal of Aerospace Research, 28*(6), 211–225.
13. Kim, J., & Park, S. (2019). High-speed aerodynamic testing of NACA 23012 airfoil in compressible flow regimes. *Journal of Aerospace Science, 17*(2), 89–105.
14. Silva, R., & Torres, M. (2020). Fatigue life estimation of NACA 23012 airfoil under cyclic loading. *Journal of Mechanical Engineering, 24*(4), 67–82.
15. Li, C., & Wang, J. (2021). Effect of wing twist distribution on NACA 23012 airfoil efficiency. *Journal of Aeronautical Engineering, 30*(1), 55–70.